Title

Base editing corrects the common Salla disease SLC17A5 c.115C>T variant

Authors

Harb, Jerry F

Christensen, Chloe L

Kan, Shih-Hsin

et al.

Publication Date

2023-12-01

DOI

10.1016/j.omtn.2023.08.024

Peer reviewed

Molecular Therapy
Nucleic Acids
Original Article

Base editing corrects the common Salla disease *SLC17A5* c.115C>T variant

Jerry F. Harb,[1] Chloe L. Christensen,[1] Shih-Hsin Kan,[1] Allisandra K. Rha,[1] Perla Andrade-Heckman,[1] Laura Pollard,[2] Richard Steet,[2] Jeffrey Y. Huang,[1] and Raymond Y. Wang[3,4]

[1]CHOC Children's Research Institute, Orange, CA 92868, USA; [2]Greenwood Genetic Center, Greenwood, SC 29646, USA; [3]Division of Metabolic Disorders, Children's Hospital of Orange County Specialists, Orange, CA 92868, USA; [4]Department of Pediatrics, University of California-Irvine School of Medicine, Irvine, CA 92697, USA

Free sialic acid storage disorders (FSASDs) result from pathogenic variations in the *SLC17A5* gene, which encodes the lysosomal transmembrane protein sialin. Loss or deficiency of sialin impairs FSA transport out of the lysosome, leading to cellular dysfunction and neurological impairment, with the most severe form of FSASD resulting in death during early childhood. There are currently no therapies for FSASDs. Here, we evaluated the efficacy of CRISPR-Cas9-mediated homology directed repair (HDR) and adenine base editing (ABE) targeting the founder variant, *SLC17A5* c.115C>T (p.Arg39Cys) in human dermal fibroblasts. We observed minimal correction of the pathogenic variant in HDR samples with a high frequency of undesired insertions/deletions (indels) and significant levels of correction for ABE-treated samples with no detectable indels, supporting previous work showing that CRISPR-Cas9-mediated ABE outperforms HDR. Furthermore, ABE treatment of either homozygous or compound heterozygous *SLC17A5* c.115C>T human dermal fibroblasts demonstrated significant FSA reduction, supporting amelioration of disease pathology. Translation of this ABE strategy to mouse embryonic fibroblasts harboring the *Slc17a5* c.115C>T variant in homozygosity recapitulated these results. Our study demonstrates the feasibility of base editing as a therapeutic approach for the FSASD variant *SLC17A5* c.115C>T and highlights the usefulness of base editing in monogenic diseases where transmembrane protein function is impaired.

INTRODUCTION

Free sialic acid storage disorders (FSASDs) are a spectrum of lysosomal storage disorders caused by the absence or malfunction of sialin, a protein encoded by the *SLC17A5* gene.[1–3] Sialin is a transmembrane protein that mediates the transport of various substrates across the lysosomal membrane. Among these substrates is sialic acid, a sugar whose function is implicated in cellular communication and structural/modulatory processes. In the lysosome, FSAs are released by the action of neuraminidase on membrane gangliosides and glycosylated proteins degraded in the lysosome.[4,5] A malfunctional sialin protein consequently results in the accumulation of FSA within the lysosome, impeding proper degradation and recycling of cellular waste components. The *SLC17A5* variant determines FSASD phenotype severity: a non-functional sialin protein results in the severe infantile sialic acid storage disease (ISSD) (MIM: 269920), while variants allowing residual sialin function, as in Salla disease (SD) (MIM: 604369), have an attenuated phenotype. Patients with FSASD have increased urinary FSA excretion and clinical findings such as coarse facial features, ataxia, developmental delays, and moderate to severe neurocognitive impairments.[1–3,6]

SLC17A5 c.115C>T (p.Arg39Cys; dbSNP: rs80338794) is a pathogenic variant that, in homozygosity, is associated with the SD phenotype. More than 80% of all reported individuals with SD have at least one c.115C>T (p.R39C) *SLC17A5* pathogenic variant,[6,7] and, because of a founder effect, nearly 95% of Finnish SD patients possess this variant.

There are no therapies approved by the U.S. Food and Drug Administration (FDA) for FSASD, with current treatment directed toward managing symptoms and enhancing quality of life.[8] As sialin is a lysosomal transmembrane protein, conventional treatments for other lysosomal storage disorders such as enzyme replacement therapy, which relies on cell-to-cell cross-correction, are not feasible. Therefore, expanding current investigative studies aimed at developing therapeutic strategies, such as those based in gene editing, is critical to curing this life-limiting disease and improving patient care.

Therapeutic strategies for genetic diseases have traditionally focused on the delivery of small molecules or functional copies of the defective gene to affected cells. Treatment has shifted recently toward the development and delivery of gene therapies[9] that use programmable nucleases to modify specific loci in the genome.[10,11] The RNA-guided endonuclease complex CRISPR-Cas9 has streamlined the generation of targeted genetic alterations. The CRISPR-Cas system has been shown to target and correct genetically inherited variants in human cells, ameliorating underlying molecular pathology.

Received 4 February 2023; accepted 23 August 2023;
https://doi.org/10.1016/j.omtn.2023.08.024.

Correspondence: Raymond Y. Wang, Division of Metabolic Disorders, Children's Hospital of Orange County Specialists, Orange, CA 92868.
E-mail: rawang@choc.org

Table 1. Variants identified in FSASD fibroblasts available from the NIGMS Human Genetic Cell Repository at the Coriell Institute for Medical Research

	Allele 1			Allele 2		
Cell lines	Nucleotide change	Predicted protein change	dbSNP#	Nucleotide change	Predicted protein change	dbSNP#
GM05520	c.548A>G	p.His183Arg	rs119491109	c.1001C>G	p.Pro334Arg	rs119491110 Verheijen et al. and Tondeur et al.[3,22]
GM05521	c.548A>G	p.His183Arg	rs119491109	–	–	
GM05522	c.1001C>G	p.Pro334Arg	rs119491110	–	–	
GM08496	c.115C>T	p.Arg39Cys	rs80338794	c.1129dupG	p.Val337Glyfs*12	novel variant
GM08497	c.115C>T	p.Arg39Cys	rs80338794	c.115C>T	p.Arg39Cys	rs80338794
GM09885	c.802_816del	p.Ser268_Asn272del	rs386833994 Lemyre at al.[35]	?	?	
GM11850	c.115C>T	p.Arg39Cys	rs80338794	c.251delC	p.Pro84Glnfs*6	novel variant
GM17488	c.1138_1139delGT	p.Val380Serfs*8	rs386833988 Aula st al.[7]	?	?	
GM17493	c.115C>T	p.Arg39Cys	rs80338794	c.802_816del	p.Ser268_Asn272del	rs386833994 Lemyre at al.[35]

-: No second variant was found in *SLC17A5* carrier parents of the proband GM05520.
?: No other pathogenic nucleotide change was identified upon sequencing of all 11 exons and their intron-exon boundaries, suggesting that the second variant might be located in a non-coding area of the gene and/or the regulatory area.

Although CRISPR-Cas9 homology directed repair (HDR) represents a novel approach to therapeutic intervention, its application has significant limitations, with the most notable issues being low efficiency of desired edit(s),[12] requirement of a donor DNA template,[13] a high frequency of unwanted insertions/deletions (indels),[14] and the potential for off-target edits.[15] To address the limitations associated with CRISPR-Cas9 HDR, adenine and cytosine base editors were developed. Rather than facilitating a double-stranded break, base editors create a nick in one genomic strand, deaminating the target adenine to inosine (read as guanine) or cytosine to uridine (read as thymidine).[16–18] Base editors have successfully produced targeted nucleotide transitions in bacteria,[19] human embryos,[20] numerous other cell types and organisms,[21] and recently in patients (NCT05398029).

Cells derived from patients with FSASD are invaluable resources for disease modeling and the assessment of potential therapeutics. Therefore, genotyping the nine cell lines banked at the Coriell Institute for Medical Research reportedly associated with FSASD (proband or relative), was imperative. Of the cells genotyped, seven unique variants were identified, including patient cells harboring the *SLC17A5* c.115C>T variant in homozygosity. These cell lines will be beneficial for classifying the FSASD severity of each variant, will contribute to variant frequency calculations, and will support the development of personalized therapeutics for FSASD.

Personalized genome editing strategies have extended precision medicine to genetic conditions like SD, with molecular tools that target the source of the pathology rather than the symptoms of the disease. Herein, we report the CRISPR-Cas9-mediated correction of the *SLC17A5* c.115C>T SD variant in patient-derived human dermal fibroblasts (GM08497) using HDR and adenine base editing (ABE). ABE of the target site gave fewer (undetectable) indels compared to HDR and effectively normalized markers of cellular pathology including FSA. Translation of this ABE strategy to *Slc17a5*$^{c.115C>T/c.115C>T}$ mouse embryonic fibroblasts (MEFs) had comparable results. These findings extend the current scope of genome editing strategies to targeted correction of pathogenic variants in transmembrane proteins and amelioration of associated cellular phenotype.

RESULTS

SLC17A5 variant detection in cell lines from patients with FSASD

We analyzed nine HDF cell lines associated with FSASD available from the NIGMS Human Genetic Cell Repository at the Coriell Institute for Medical Research through Sanger sequencing of the 11 exons and respective intron-exon boundaries of the *SLC17A5* gene. Of the nine cell lines, one (GM08497) was found to harbor the *SLC17A5* c.115C>T (p.Arg39Cys) variant in homozygosity. Three cell lines, GM05520-22, were derived from a Yugoslavian family of a proband presenting with ISSD initially reported in 1982.[22] The cell line derived from the proband (GM05520) was reported as compound heterozygous for c.548A>G (p.His183Arg; dbSNP: rs119491109) and c.1001C>G (p.Pro334Arg; dbSNP: rs119491110) variants in *SLC17A5*.[3,22] The carrier status of each parent, GM05521 and GM05522, is elucidated here (Table 1).

A previously reported 15-bp deletion in exon 6 of *SLC17A5* (c.802_816del; p.Ser268_Asn272del; dbSNP: rs386833994) was found in heterozygosity in both GM17493 and GM09885. GM17493 was found to be compound heterozygous for the c.115C>T variant. Interestingly, a second pathogenic variant was not identified in GM09885. This suggests that the second pathogenic variant may be in a regulatory region or other non-coding region. Similarly, only one *SLC17A5* variant (c.1138_1139delGT; p.Val380Serfs*8; dbSNP: rs386833988)

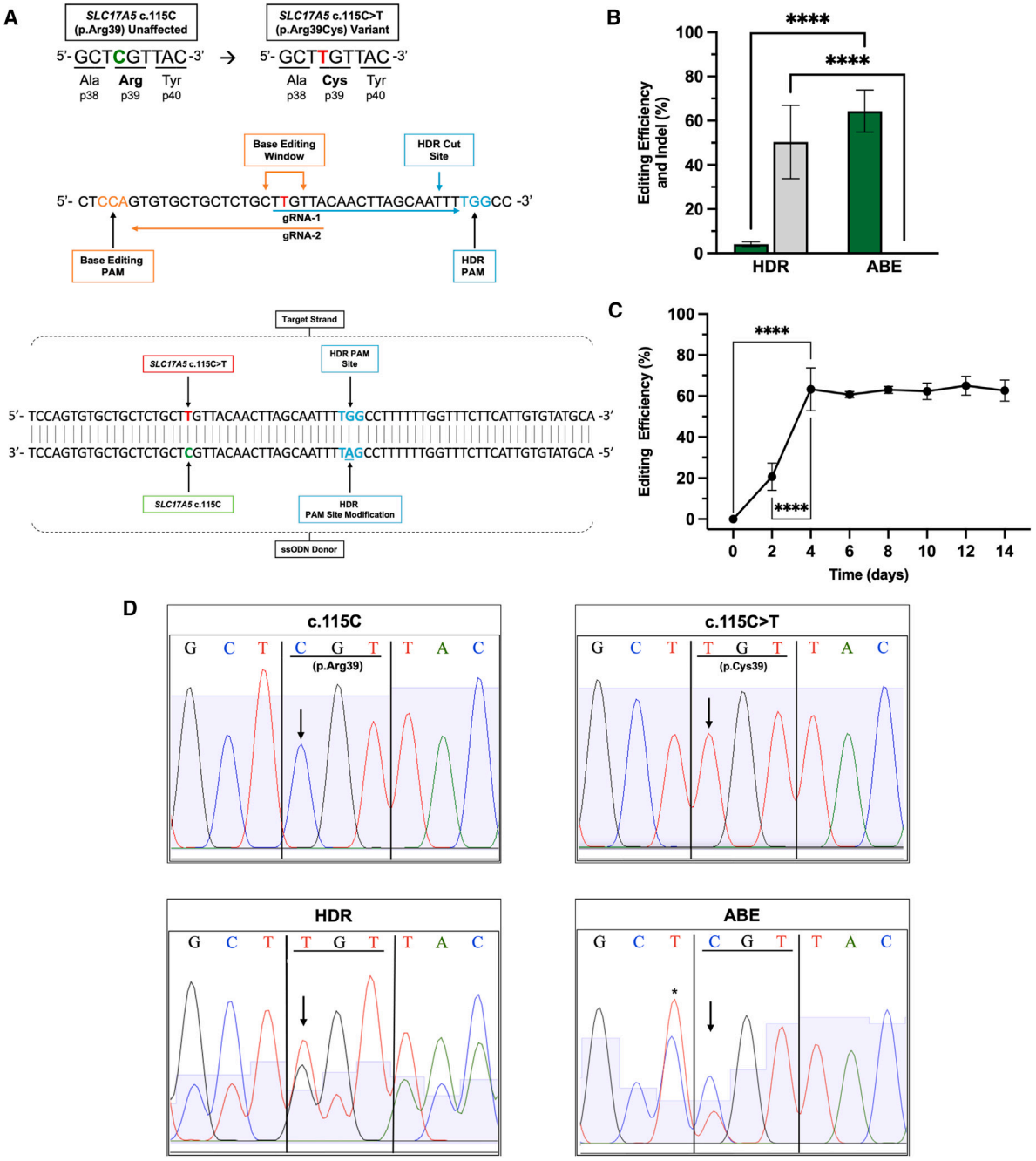

Figure 1. ABE restores *SLC17A5* c.115C sequence without creating indels in HDFs

(A) DNA and respective protein sequences of *SLC17A5* around locus c.115. (Top left) c.115C site (in green) and CGT coding for arginine at codon 39 of the SLC17A5 protein. (Top right) pathogenic variant *SLC17A5* c.115C>T (in red), coding for cysteine at codon 39 of the SLC17A5 protein. (Middle) sgRNA design for HDR and ABE. The *SLC17A5* c.115 site for the targeted cytosine-to-thymine transition is highlighted in red. Horizontal arrows indicate sequences of sgRNAs targeting the *SLC17A5* c.115 site. Protospacer adjacent motifs (PAMs) are highlighted in color corresponding with the respective sgRNA: for HDR, in blue, and base editing, in orange. (Bottom) Sequence of single-stranded oligonucleotide (ssODN) used for HDR around *SLC17A5 c*.115C>T. PAM motifs are indicated in blue. A synonymous substitution to inactivate the PAM site (*SLC17A5* c.135G>A) is underlined. (B) Comparison of editing efficiency (green) and indel (gray) (%) between HDR and ABE in HDFs harboring the *SLC17A5* c.115C>T variant (affected). (C) Temporal assessment of editing efficiency in HDFs following base editing from day zero to day 14 post-nucleofection. (D) Electropherograms of *SLC17A5* sequence flanking c.115 in unaffected control, affected, HDR-treated, and ABE-treated HDFs, respectively. Shaded blue regions in the background of chromatograms represent Phred base calling quality scores. *SLC17A5* c.115 site distinguished by arrows. (Top left) *SLC17A5* c.115 unaffected control HDFs. Note the canonical

(legend continued on next page)

was identified in GM17488. This variant has been reported in compound heterozygosity with the c.115C>T variant in patients with severe SD.[7] However, in the GM17488 cell line, no c.115C>T variant in *SLC17A5* was observed. Furthermore, we identified two novel *SLC17A5* variants, c.251delC (p. Pro84Glnfs*6) and c.1129dupG (p.Val337Glyfs*12), in GM11850 and GM08496, respectively. Both cell lines are also compound heterozygous for the *SLC17A5* c.115C>T variant. Analysis of the GM11850 cell line revealed two variants in exon 2. Subsequent analysis by allele-specific PCR identified the phase of two variants, c.251delC and c.115C>T, as *trans*. In this study, both GM08497 (homozygous *SLC17A5* c.115C>T variants) and GM11850 (compound heterozygous with one *SLC17A5* c.115C>T variant) were used for subsequent genome editing experiments.

HDR of *SLC17A5* c.115C>T results in minimal editing efficiency

Single guide RNA (sgRNA)-1 (Figure 1A) was designed for HDR using the online design tool CRISPick.[23] A single-stranded HDR template with 70 nucleotide homology arms was designed to incorporate c.115C and install a silent PAM site modification (Figure 1A). CRISPR-Cas9 HDR targeting of this genomic site in HDFs yielded a low editing efficiency (4.1% ± 1.1%) while generating a high percentage of indels (50.3% ± 16.6%) (Figure 1B).

Editing efficiency and specificity is improved with ABE over HDR

We selected a sgRNA (sgRNA-2), located on the antisense strand, to target the c.115 'C' to 'T' transition on the sense strand (Figure 1A). Base editing of the c.115C>T target variant was observed in HDFs 4 days post-transfection with an average editing efficiency of 64.3% ± 9.6% and no detected indels (Figure 1B). Peak editing efficiency is achieved at 4 days after transfection, after which efficiency plateaus until at least 14 days after transfection (Figure 1C). Of note, transfected HDFs were found to have a bystander edit (c.114T>C) that occurs at a frequency 27.6% ± 15.8%. This bystander edit results in a p.Ala38Ala synonymous substitution not predicted to impact protein function (Figure 1D).

ABE-treated *SLC17A5* c.115C>T HDFs show nonsignificant reductions in lysosomal-associated membrane protein 1 and CD63

Lysosomal-associated membrane protein 1 (LAMP1) is a commonly used marker for lysosome storage. CD63 is a membrane-associated protein present on compartments of the endo-lysosomal pathway. Both LAMP1 and CD63 levels are expected to be present in higher abundance with increased lysosome burden. Immunocytochemistry (ICC) of LAMP1 and CD63 was performed for unaffected control HDFs, untreated homozygous *SLC17A5* c.115C>T HDFs, and ABE-treated *SLC17A5* c.115C>T HDFs (Figures 2A, 2C, and S1–S6). ABE-treated HDFs demonstrate a nonsignificant, but downward trend in LAMP1 (0.21 mean intensity units [miu] vs. 0.16 miu, $p = 0.13$) and CD63 (0.17 miu vs. 0.13 miu, $p = 0.06$) levels when compared with affected HDFs (Figures 2B and 2D).

Western blot analysis of LAMP1 and CD63 revealed no significant differences across affected, ABE-treated, and unaffected control conditions when normalized to loading controls (Figure S7).

FSA levels are reduced in ABE-treated *SLC17A5* c.115C>T HDFs

We observed increased FSA levels in untreated homozygous *SLC17A5* c.115C>T HDFs (3.07 nM/mg protein) compared with unaffected control HDFs (1.43 nM/mg protein). ABE-treated *SLC17A5* c.115C>T HDFs (1.33 nM/mg protein) demonstrated a significant reduction of FSA compared with untreated *SLC17A5* c.115C>T HDFs and shows normalization to unaffected control levels (Figure 2E).

FSA levels in a different FSASD patient HDF line (GM11850) with compound heterozygous variants in *SLC17A5* (c.115C>T/c.251delC) were also elevated (9.32 nM/mg protein) and was significantly reduced in ABE-treated samples (2.85 nM/mg protein) (Figure S8). ABE-treated compound heterozygote samples produced an editing efficiency of 99% with minimal to no detectable indels.

Deep sequencing of *in silico*-nominated off-target sites does not show off-target editing above baseline levels

In silico off-target analysis of the *SLC17A5* c.115C>T-targeting sgRNA was conducted to determine the frequency of putative off-target sites using Cas-OFFinder.[24] Sites were initially characterized using a mismatch parameter of five or fewer nucleotides, identifying 1,192 sites (Figure 3). A more stringent three nucleotide mismatch maximum identified 15 predicted off-target sites which were defined as either intergenic, intronic, long non-coding RNA, or as a pseudogene (Figure 3B). To determine the potential impact of off-target editing, we performed targeted amplicon deep sequencing on genomic DNA isolated from ABE-treated and mock HDFs. Of the 15 sites, two intergenic sites (OT2 and OT10) contained highly repetitive sequences and could not be amplified for deep sequencing (Tables S2 and S3). Deep sequencing reads were analyzed using CRISPResso2,[25] resulting in 11/13 off-target sites with >1,000× coverage. No detectable off-target editing above baseline levels was evident across these 11 putative off-target sites (Figures 3C and S9).

Base editing corrects *Slc17a5* c.115C>T in MEFs

To demonstrate base editing translatability to a murine model of SD, a MEF cell line possessing the c.115C>T variant in *Slc17a5* was transfected with an ABE and a *Slc17a5* c.115C>T-targeting sgRNA (sgRNA-3) (Figure 4A). Sanger sequencing of *Slc17a5* post-transfection shows an average editing efficiency of 66.4% ± 9.9%, comparable with

'C' nucleotide at position c.115. (Top right) Homozygous *SLC17A5* c.115C>T variant HDFs. Note the mutated 'T' nucleotide at position c.115. (Bottom left) HDR-treated *SLC17A5* c.115C>T HDFs. Multiple electropherogram peaks indicative of indels. (Bottom right) ABE-treated *SLC17A5* c.115C>T affected HDFs. Note the dual peak for 'T' and 'C', indicating partial correction of the pathogenic 'T' to the canonical 'C' nucleotide at c.115. Bystander edit at c.114 is marked with an asterisk. Data generated from at least three independent experiments are shown as mean ± standard deviation. Editing efficiency (%) and indel (%) were analyzed using unpaired t tests. Temporal assessment was analyzed using one-way ANOVA with the Tukey *post hoc* test. ****$p < 0.0001$.

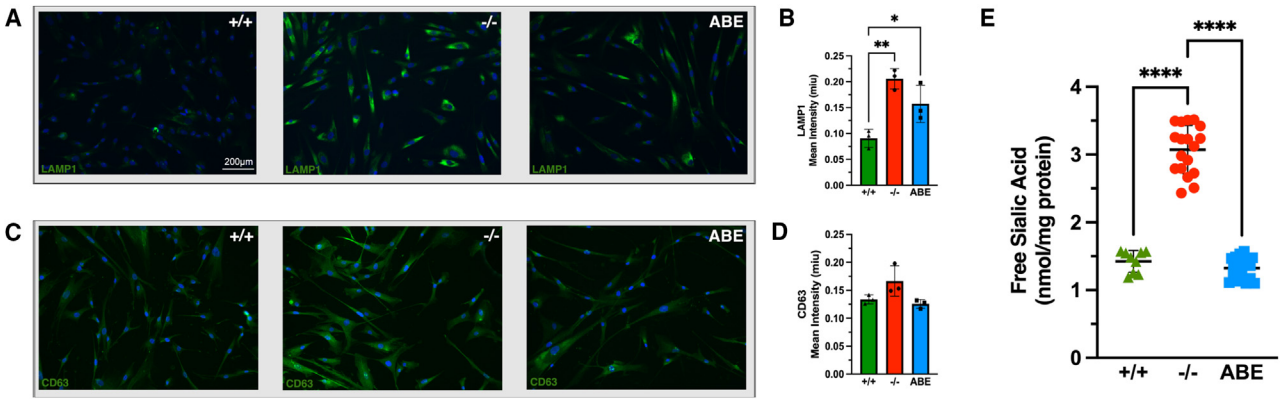

Figure 2. ABE reduces markers of endo-lysosomal pathology and normalizes FSA levels in HDFs

(A and C) LAMP1(A) and CD63 (C) staining in unaffected control (+/+), affected homozygous *SLC17A5* c.115C>T (−/−), and ABE-treated *SLC17A5* c.115C>T HDFs (ABE). Scale bar, 200 μm. (B and D) Quantification of LAMP1 (B) and CD63 (D) signal intensity in HDFs, measured in mius. The editing efficiency of the ABE-treated group used for staining corresponds with 53%. (E) Quantification of FSA in HDFs. Increased FSA levels in untreated affected HDFs (−/−) compared to unaffected control HDFs (+/+). Data generated from at least (n = 3) independent experiments are shown as mean ± standard deviation. All comparisons were analyzed using a one-way ANOVA with the Tukey post-hoc test. *p < 0.05; **p < 0.01; ****p < 0.0001. See also Figures S1– S8.

the observed editing efficiency in HDFs (64.3% ± 9.6%) (Figure 4B). FSA levels in affected *Slc17a5* c.115C>T MEFs were significantly increased (11.59 nM/mg protein) in comparison with unaffected control MEFs (0.48 nM/mg protein), while the FSA levels in ABE-treated *Slc17a5* c.115C>T MEFs were significantly decreased (1.33 nM/mg protein) compared with untreated *Slc17a5* c.115C>T MEFs and shows normalization to unaffected control levels (Figure 4C).

DISCUSSION

We present the first genome editing study in cells derived from patients carrying the common SD *SLC17A5* c.115C>T variant.[7,26] Since SD has no FDA-approved therapy, this study begins to address a significant unmet need for patients, generating vital proof-of-principle results for the optimization of an ABE-based therapeutic strategy. Given that 80% of SD patients harbor at least one *SLC17A5* c.115C>T variant, successful implementation of ABE-mediated c.115C>T correction may benefit a large proportion of SD patients worldwide.

In this work, we demonstrated that ABE generated superior correction of the target allele when compared with HDR, and that using an ABE-mediated strategy produced improvements in markers of disease pathology in treated cells. This improvement is evident through molecular analysis, with an average of 64.3% ± 9.6% correction of the pathogenic variant to the canonical c.115C. This level of correction is reached four days following nucleofection and is sustained over time (Figure 1C). With the exception of the synonymous bystander edit c.114T>C (p.Ala38Ala), we did not identify any off-target edits or indels (Figures 3 and S9, and Table S2). Since there is an increase in codon usage frequency between GCT (0.26) and GCC (0.40), we do not expect there to be a negative impact on protein translation due to editing of c.114 (Figures 1A and 1D). Although we do not predict the *SLC17A5* c.114 bystander will affect sialin function, we plan to investigate this variant further *in vitro*.

In ABE-treated samples, cells displayed a nonsignificant reduction of LAMP1 and CD63, markers of cellular lysosomal burden by ICC. For both proteins, we observed a trend of reduced signal intensity in ABE-treated c.115C>T HDFs compared with untreated c.115C>T HDFs (Figures 2A–2D and S1–S6). Given that the model evaluated in this study was HDFs, and not a cell type (e.g., neurons or glial cells) likely impaired by FSA storage, we hypothesize that there may be a limited lysosomal storage phenotype, as evidenced by inconclusive results in LAMP1 and CD63 signal intensity across ABE-treated, untreated c.115C>T, and unaffected HDFs upon western blotting (Figure S7). Cellular models of SD that recapitulate disease pathology, including those of the CNS, would better support measures of efficacy in ABE-treated samples.

FSA levels in unaffected control, untreated c.115C>T, and ABE-treated c.115C>T HDFs support our assertion that successful base editing reduced lysosomal storage in affected HDFs. While FSA in untreated *SLC17A5* c.115C>T HDFs is significantly elevated compared with unaffected controls, ABE-treated homozygous c.115C>T HDFs demonstrated near-normalization of FSA (Figure 2E). These data suggest that functional sialin protein is produced in ABE-treated HDFs. The observation of significantly reduced FSA in an ABE-treated c.115C>T/c.251delC HDF line in which more than 99% of the target allele is corrected (Figure S8) supports this conclusion, indicating that correction of only one allele is sufficient to restore sialin function and lysosomal FSA efflux. This is exceptionally relevant for translation of our strategy to the SD population, where c.115C>T is the predominant pathogenic allele.

Evaluating the safety and efficacy of the defined ABE strategy in an animal model of SD is an important next step. Initial translation of this strategy to *Slc17a5*$^{c.115C>T/c.115C>T}$ MEFs showed no cross-species

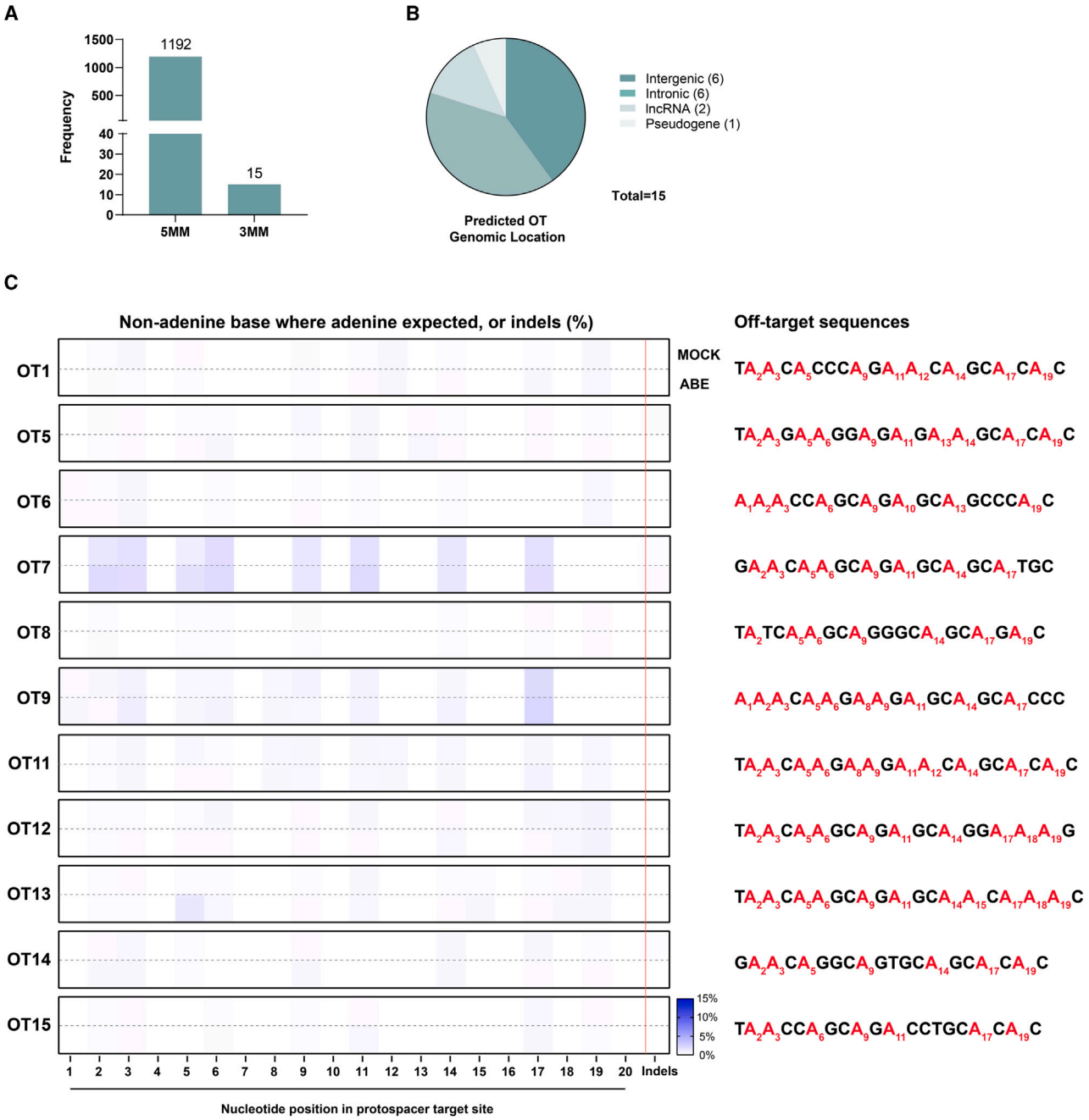

Figure 3. Targeted amplicon deep sequencing of putative off-target sites nominated *in silico* show no significant adenine deamination

Putative off-target (OT) sites were determined by Cas-OFFinder[24] using the c.115T 20-nucleotide query sequence. (A) OT site frequencies predicted by the Cas-OFFinder algorithm using a mismatch parameter of five or fewer nucleotides (5MM) compared with three or fewer nucleotides (3MM). (B) Predicted OT sites separated by genomic location type, with a majority of predicted OTs found to be in intergenic or intronic regions. (C) Heatmap (left) representing percentage of non-adenine base identities where adenine is expected, or indels (right), across *in silico*-nominated off-target sites after targeted amplicon deep sequencing and CRISPResso2 analysis.[25] No significant differences are observed between ABE-treated *SLC17A5* c.115C>T HDFs (ABE; bottom) and mock (top) samples. Associated OT sequences are listed at right, and adenines with the potential for deamination are in red (n = 3, unpaired Student t tests). See also Tables S2 and S3, Figures S9 and S10.

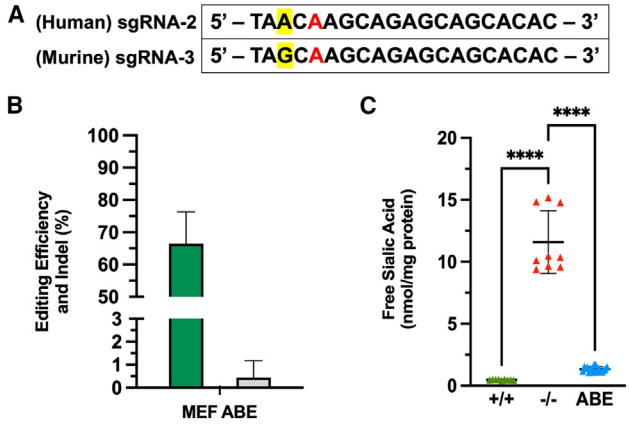

Figure 4. ABE restores *Slc17a5* c.115C in a murine cell line

(A) Human and murine sgRNA comparison. Murine and human sequences are identical, except a single nucleotide difference, highlighted in yellow. *SLC17A5/Slc17a5* c.115C>T is in red. (B) Base-editing efficiency (green) and indel (gray) (%) MEFs harboring the *SLC17A5* c.115C>T variant. (C) FSA quantification in MEFs. Increased FSA levels in untreated *Slc17a5* c.115C>T MEFs (–/–) compared to unaffected control MEFs (+/+). ABE-treated *Slc17a5* c.115C>T MEFs (ABE) demonstrate normalization of FSA. Data generated from at least (n = 3) independent experiments are shown as mean ± standard deviation. All comparisons were analyzed using a one-way ANOVA with the Tukey *post hoc* test. ****$p < 0.0001$.

efficacy of either sgRNA (Figure 4A) despite differing by only one nucleotide within the target region. Base editing of the *Slc17a5* c.115C>T site using murine-specific sgRNA-3 was successful in *Slc17a5* c.115C>T MEFs (Figure 4B) and resulted in a significant reduction of cellular FSA to normal levels (Figure 4C) suggesting that genomic correction effectively restored sialic acid metabolism. We plan to evaluate whether intra-cranially-delivered ABE and sgRNA-3 results in efficacious correction of the *Slc17a5* c.115C>T pathogenic variant in hippocampal and Purkinje cells, as well as oligodendrocytes and astrocytes, in the murine model of SD (unpublished). We will assess for reduction of cellular pathology and FSA levels, and whether potential correction at the molecular and cellular level translates to any benefits in longevity, motor function, and cognition in *Slc17a5*$^{c.115C>T/c.115C>T}$ mice.

While genotyping the FSASD patient cells from the NIGMS Human Genetic Cell Repository at the Coriell Institute for Medical Research, two variants in *SLC17A5* not previously reported in the literature were identified: c.251delC (p.Pro84Glnfs*6) and c.1129dupG (p.Val337Glyfs*12) in GM11850 and GM08496, respectively (Table 1). Sanger sequencing of the *SLC17A5* cDNA from these cell lines was performed and neither variant was detected, suggesting nonsense-mediated decay may be responsible. The potential pathogenic burden of these variants is likely loss of function, but further characterization is required to determine the respective impact. Functional consequences of these variants are unknown, yet potential differences in the protein structure, respective to these novel variants, suggests possible changes to protein stability and/or activity.[27]

Importantly, not all FSASD pathogenic variants are targetable by base editing. The genomic context with respect to the type of variant, PAM site flexibility, base editing window rigidity, and predicted impact of bystander editing will limit candidates. For those variants where base editing is not feasible, including the novel variants identified herein, prime editing may be used.

To further support the evaluation of the safety and efficacy of this ABE strategy, it is imperative that a comprehensive unbiased analysis of off-targets *in vitro*, such as CIRCLE-seq, be conducted before therapeutic translation.[28] Future studies will also elucidate the subcellular localization of ABE-treated sialin and the role of existing cellular pathophysiology, such as autophagic dysregulation, on sialin trafficking.

MATERIALS AND METHODS

Cell culture, maintenance, and cell lines

HDF cell lines were obtained from the NIGMS Human Genetic Cell Repository at the Coriell Institute for Medical Research Inc., and from the American Type Culture Collection (ATCC). Cells were cultured in DMEM (Cytiva) supplemented with 15% fetal bovine serum (Omega Scientific), 2 mM GlutaMAX (Gibco), and 1% antibiotic-antimycotic (100 U/mL penicillin, 100 μg/mL streptomycin, and 0.25 μg/mL amphotericin B; Gibco). A MEF cell line from a *Slc17a5*$^{c.115C>T/c.115C>T}$ mouse model was provided as a generous gift from Drs. Marjan Huizing and May Malicdan at the National Human Genome Research Institute.[29] MEF cells were cultured on 0.1% gelatin-coated plates in HDF culture medium supplemented with 1× MEM non-essential amino acids (MEM NEAA; Gibco) and 12.87 mM β-mercaptoethanol (Gibco). All cell lines were maintained at 37°C/5% CO_2 air atmosphere until reaching optimal confluency of 85%–90% for nucleofection.

Genomic analysis for novel variant identification

Genomic DNA was extracted from each cell line using QuickExtract DNA Extraction Solution (LGC Biosearch Technologies). *SLC17A5* sequence analysis was conducted using previously established intronic primers that flank each side of the exon.[7] Minor modifications to the primer design of some exons are listed in the supplemental information (Table S1). PCR products were purified using the DNA Clean & Concentrator-5 kit (Zymo Research) before Sanger sequencing with both forward and reverse primers, resulting in complete coverage of the amplified regions (Eurofins Genomics). Analysis of the GM11850 cell line revealed two heterozygous changes in exon 2, and therefore a set of allele-specific oligos (C115: 5′- CAG TGTGCTGCTCTGCT**C**-3′ and T115: 5′- CAGTGTGCTGCTCTG CT**T**-3′) was designed to identify the relative allelic position between c.251delC and c.115C>T in *SLC17A5*.

SLC17A5 c.115 sgRNA and single-stranded oligonucleotide design

All oligonucleotides used in this study were synthesized by Integrated DNA Technologies. CRISPR-Cas9 sgRNAs targeting the *SLC17A5* c.115 site, used in the application of CRISPR-Cas9 HDR, were

generated using *in silico* design tool CRISPick,[23] which provided prospective sgRNAs maximizing on-target activity and minimizing off-target effects. Single-stranded oligonucleotides with 70 nucleotide homology arms flanking the target site and a synonymous substitution in the PAM, were used together with sgRNA-1 to facilitate genomic correction. sgRNAs directing *SLC17A5* c.115 base editing were generated using *in silico* design tool BE-Designer.[30] Prospective sgRNAs were chosen based on the information provided by the BE-Designer tool: CRISPR-Cas9 orthologue, base editing activity windows, G-C content, potential mismatches, and off-target sites.

SLC17A5 c.115 base editing sgRNA expression vector cloning

SLC17A5 c.115-specific sgRNA oligonucleotides with *Bsm*BI restriction enzyme overhangs were designed as follows: forward oligo (5′-CACC(sgRNA)-3′); reverse oligo (5′-AAAC(reverse complement sgRNA)-3′). Complementary sgRNA oligonucleotides were annealed and ligated to *Bsm*BI-digested BPK1520 plasmid using the Quick Ligation Kit (New England Biolabs). BPK1520 was a gift from Keith Joung (Addgene plasmid #65777; http://n2t.net/addgene:65777; RRID: Addgene_65777).[31] NEB 5α competent *Escherichia coli* (New England Biolabs) were transformed with ligated plasmid DNA using standard protocol. Individual colonies were confirmed by Sanger sequencing, and sgRNA-containing plasmid DNA was purified using a ZymoPURE II Plasmid Midiprep Kit (Zymo research).

Nucleofection

Cells were transfected using the Lonza nucleofection system (4D-Nucleofector Core Unit, Lonza) with program CA-137. For HDR, 8–9 × 10^4 *SLC17A5* c.115C>T HDFs carrying *SLC17A5* c.115C>T allele(s) (GM08497) were transfected in SE Cell Solution (Lonza) with 30 μM *SLC17A5* c.115-specific RNP and 50–250 pM donor single-stranded oligonucleotide. For base editing, 8–9 × 10^4 *SLC17A5* c.115C>T homozygous HDFs (GM08497 and GM11850) were transfected in P2 Primary Cell Solution (Lonza) with 250 ng BPK1520-*SLC17A5* c.115 sgRNA expression vector and 750 ng pCMV_ABEmax_P2A_GFP. pCMV_ABEmax_P2A_GFP was a gift from David Liu (Addgene plasmid #112101; http://n2t.net/addgene:112101; RRID: Addgene_112101).[32] Editing efficiency was determined using the Synthego ICE Analysis tool (Synthego Performance Analysis, ICE Analysis. 2019. v3.0).

ICC analysis

For determination of LAMP1 and CD63 signal by fluorescence microscopy, unaffected control (HDFs, PCS-201-010; ATCC), affected *SLC17A5* c.115C>T (GM08497), and ABE-treated *SLC17A5* c.115C>T HDFs were grown on eight-chamber cell culture slides (CellTreat Scientific Products). Cells were fixed with zinc sulfate formalin (Mercedes Scientific), and permeabilized in 100% ethanol before blocking in 1% BSA. Primary antibodies (rabbit against LAMP1; 1:200; Abcam, RRID:AB_775978) or (rabbit against CD63; 1:100; R&D Systems; RRID: AB_2927414) was applied for 1 h at 37°C before applying secondary antibody (donkey anti-rabbit IgG (H + L)-AF488; 1:500–1,000; Molecular Probes; RRID: AB_2535792) for 1 h at 37°C. Slides were mounted using VECTASHIELD antifade mounting medium with DAPI (Vector Laboratories). Images were captured on the Keyence BZ-X800 imaging system at 20× magnification. The exposure time for GFP (AF488) and DAPI are 1 s and 0.01 s, respectively. Quantification of LAMP1 and CD63 signal intensity was performed using CellProfiler[33] by establishing a module pipeline which included "IdentifyPrimaryObjects" and "MeasureObjectIntensity."

Western blot analysis

Unaffected control (n = 3), affected (n = 3), and ABE-treated (n = 3) HDF cell pellets were lysed in CelLytic M (Sigma-Aldrich), and protein concentration was estimated by BCA assay (ThermoFisher Scientific). A total of 8 μg protein was resolved in 4%–15% mini-PROTEAN TGX Stain-Free gels (Bio-Rad) and transferred to PVDF membranes using the Tran-Blot Turbo Transfer System (Bio-Rad) Membranes were then blocked in 2% casein for 1 h before overnight incubation with one of the following primary antibodies: LAMP1 mouse monoclonal antibody (1:1,000, Abcam; RRID: AB_470708) or CD63 mouse monoclonal antibody (1:1,000, Santa Cruz Biotechnology; RRID: AB_627877). Loading controls for LAMP1 and CD63 are GAPDH (1:2,500, Novus Biologicals; RRID: AB_10002458) and Vinculin (1:1,000, Cell Signaling Technology; RRID: AB_2728768) antibodies, respectively. Secondary antibody (anti-mouse-HRP Bio-Rad; RRID: AB_11125547; anti-rabbit-HRP, Bio-Rad Anti-Rabbit-HRP; RRID: AB_11125142 all 1:3,000) were applied to the membrane at room temperature for 45 min. Clarity Western ECL Substrate (Bio-Rad 170-5060) was applied and ECL signals were captured by Bio-Rad ChemiDoc Imaging System and quantified with FIJI software.[34]

FSA quantification assay

Lysate containing approximately 1 × 10^6 cells was mixed with deuterated internal standard and four volumes of HPLC-grade water. Samples were filtered using a Spin-X 0.22-mm microcentrifuge filter tube. FSA was analyzed by UPLC-MS/MS (Waters Acquity I-Class; Xevo TQ-S MS/MS), using a C18 reverse-phase column (Waters Acquity UPLC HSS T3) for chromatographic separation and tandem mass spectrometry operated in selected reaction monitoring mode (electrospray ionization, positive ion mode) for detection. Quantification was accomplished by stable isotope dilution and comparison to a standard curve. FSA concentrations were normalized by total protein concentration as determined by the Lowry method. The limit of quantification for FSA was 0.1 μM/L. All sample runs demonstrated calibration curves with linearity exceeding $r^2 > 0.99$.

Off-target analysis

In silico prediction of putative off-target sites was performed using Cas-OFFinder with a query sequence of TAACAAGCAGAG CAGCACAC and an NGG protospacer adjacent motif, allowing for up to three mismatches between the query sequence and genomic off-target site. Genomic DNA extracted from ABE-treated (n = 3) and mock (n = 3) HDFs was PCR amplified with Taq RED (Apex Bioresearch Products) using site-specific primers (Table S2), generating fewer than 250 bp amplicons. Amplified DNA was electrophoresed

on 0.7% agarose gels in TAE buffer, size selected, and gel purified using the Zymoclean Gel DNA Recovery Kit (Zymo Research). Amplicons were library prepped using the NEBNext Ultra II DNA Library Prep kit (New England Biolabs), according to the manufacturer's protocol. Size selection of adaptor-ligated DNA was performed using AMPure XP beads (Beckman Coulter) using a bead/sample ratio of 0.7×. Adaptor-ligated DNA was enriched using universal and index primers, as per manufacturer's protocol, with five PCR cycles. Libraries were run paired end on a MiSeq (Illumina) using the MiSeq Reagent Kit v2 Nano (Illumina) with 500 cycles generating more than 18,000 NGS reads/index primer, more than 1,000× reads/sample. One or both read files (.fastq) were analyzed using CRISPResso2 (Figure S10).[25]

Statistical analysis

Statistical analyses and graphing were carried out in GraphPad Prism (Prism Version 8 for Windows 64-bit).

DATA AND CODE AVAILABILITY

All data are available in the article. Correspondence and requests for materials should be addressed to RYW. Reprints and permissions information is available.

SUPPLEMENTAL INFORMATION

Supplemental information can be found online at https://doi.org/10.1016/j.omtn.2023.08.024.

ACKNOWLEDGMENTS

Homozygous *Slc17a5* c.115C>T (p.Arg39Cys) MEFs were provided to as a generous gift from Drs. Marjan Huizing and May Malicdan at the NHGRI.[29] This work was made possible, in part, through access to the Genomics Research and Technology Hub (formerly Genomics High-Throughput Facility) Shared Resource of the Cancer Center Support Grant (P30CA062203), the Single Cell Analysis Core shared resource of Complexity, Cooperation and Community in Cancer (U54CA217378), the Genomics-Bioinformatics Core of the Skin Biology Resource Based Center @ UCI (P30AR075047) at the University of California, Irvine and NIH shared instrumentation grants 1S10RR025496-01, 1S10OD010794-01, and 1S10OD021718-01. This work was supported by the Campbell Foundation of Caring, The Larry and Helen Hoag Foundation, and a CHOC One Wish Grant.

AUTHOR CONTRIBUTIONS

Conceived ideas or experimental design of study: J.F.H., J.Y.H., S.H.K., R.Y.W., C.C., and A.K.R.; performed experiments/data collection: J.F.H., S.H.K., C.C., A.K.R., P.A.H., R.S., and L.P.; data analysis/interpretation: J.F.H., S.H.K., C.C., A.K.R., P.A.H., R.S., L.P., J.Y.H., and R.Y.W.; primary author: J.F.H.; provided revisions to scientific content of manuscript: S.H.K., C.C., A.K.R., P.A.H., R.S., L.P., and R.Y.W.; principal investigator: R.Y.W.

DECLARATION OF INTERESTS

There are no competing interests to disclose.

REFERENCES

1. Aula, P., Autio, S., Raivio, K.O., Rapola, J., Thodén, C.J., Koskela, S.L., and Yamashina, I. (1979). "Salla disease": a new lysosomal storage disorder. Arch. Neurol. *36*, 88–94. https://doi.org/10.1001/archneur.1979.00500380058006.

2. Renlund, M., Aula, P., Raivio, K.O., Autio, S., Sainio, K., Rapola, J., and Koskela, S.L. (1983). Salla disease: a new lysosomal storage disorder with disturbed sialic acid metabolism. Neurology *33*, 57–66. https://doi.org/10.1212/wnl.33.1.57.

3. Verheijen, F.W., Verbeek, E., Aula, N., Beerens, C.E., Havelaar, A.C., Joosse, M., Peltonen, L., Aula, P., Galjaard, H., van der Spek, P.J., and Mancini, G.M. (1999). A new gene, encoding an anion transporter, is mutated in sialic acid storage diseases. Nat. Genet. *23*, 462–465. https://doi.org/10.1038/70585.

4. Qin, L., Liu, X., Sun, Q., Fan, Z., Xia, D., Ding, G., Ong, H.L., Adams, D., Gahl, W.A., Zheng, C., et al. (2012). Sialin (SLC17A5) functions as a nitrate transporter in the plasma membrane. Proc. Natl. Acad. Sci. USA *109*, 13434–13439. https://doi.org/10.1073/pnas.1116633109.

5. Wreden, C.C., Wlizla, M., and Reimer, R.J. (2005). Varied mechanisms underlie the free sialic acid storage disorders. J. Biol. Chem. *280*, 1408–1416. https://doi.org/10.1074/jbc.M411295200.

6. Huizing, M., Hackbarth, M.E., Adams, D.R., Wasserstein, M., Patterson, M.C., Walkley, S.U., Gahl, W.A., Dobrenis, K., Foglio, J., Gasnier, B., et al. (2021). Mini-Review Free Sialic Acid Storage Disorder: Progress and Promise (Neurosci Lett), 135896. https://doi.org/10.1016/j.neulet.2021.135896.

7. Aula, N., Salomäki, P., Timonen, R., Verheijen, F., Mancini, G., Månsson, J.E., Aula, P., and Peltonen, L. (2000). The spectrum of SLC17A5-gene mutations resulting in free sialic acid-storage diseases indicates some genotype-phenotype correlation. Am. J. Hum. Genet. *67*, 832–840. https://doi.org/10.1086/303077.

8. Adams, D., and Wasserstein, M. (2003). Free Sialic Acid Storage Disorders. In GeneReviews®, M. Adam, H. Ardinger, and R. Pagon, eds. (University of Washington).

9. Gupta, R.M., and Musunuru, K. (2014). Expanding the genetic editing tool kit: ZFNs, TALENs, and CRISPR-Cas9. J. Clin. Invest. *124*, 4154–4161. https://doi.org/10.1172/JCI72992.

10. Carroll, D. (2011). Genome engineering with zinc-finger nucleases. Genetics *188*, 773–782. https://doi.org/10.1534/genetics.111.131433.

11. Urnov, F.D., Rebar, E.J., Holmes, M.C., Zhang, H.S., and Gregory, P.D. (2010). Genome editing with engineered zinc finger nucleases. Nat. Rev. Genet. *11*, 636–646. https://doi.org/10.1038/nrg2842.

12. Zhang, J.P., Li, X.L., Li, G.H., Chen, W., Arakaki, C., Botimer, G.D., Baylink, D., Zhang, L., Wen, W., Fu, Y.W., et al. (2017). Efficient precise knockin with a double cut HDR donor after CRISPR/Cas9-mediated double-stranded DNA cleavage. Genome Biol. *18*, 35. https://doi.org/10.1186/s13059-017-1164-8.

13. Lin, S., Staahl, B.T., Alla, R.K., and Doudna, J.A. (2014). Enhanced homology-directed human genome engineering by controlled timing of CRISPR/Cas9 delivery. Elife *3*, e04766. https://doi.org/10.7554/eLife.04766.

14. Cullot, G., Boutin, J., Toutain, J., Prat, F., Pennamen, P., Rooryck, C., Teichmann, M., Rousseau, E., Lamrissi-Garcia, I., Guyonnet-Duperat, V., et al. (2019). CRISPR-Cas9 genome editing induces megabase-scale chromosomal truncations. Nat. Commun. *10*, 1136. https://doi.org/10.1038/s41467-019-09006-2.

15. Cho, S.W., Kim, S., Kim, Y., Kweon, J., Kim, H.S., Bae, S., and Kim, J.S. (2014). Analysis of off-target effects of CRISPR/Cas-derived RNA-guided endonucleases and nickases. Genome Res. *24*, 132–141. https://doi.org/10.1101/gr.162339.113.

16. Komor, A.C., Kim, Y.B., Packer, M.S., Zuris, J.A., and Liu, D.R. (2016). Programmable editing of a target base in genomic DNA without double-stranded DNA cleavage. Nature *533*, 420–424. https://doi.org/10.1038/nature17946.

17. Gaudelli, N.M., Komor, A.C., Rees, H.A., Packer, M.S., Badran, A.H., Bryson, D.I., and Liu, D.R. (2017). Programmable base editing of A·T to G·C in genomic DNA without DNA cleavage. Nature *551*, 464–471. https://doi.org/10.1038/nature24644.

18. Nishida, K., Arazoe, T., Yachie, N., Banno, S., Kakimoto, M., Tabata, M., Mochizuki, M., Miyabe, A., Araki, M., Hara, K.Y., et al. (2016). Targeted nucleotide editing using hybrid prokaryotic and vertebrate adaptive immune systems. Science *353*, aaf8729. https://doi.org/10.1126/science.aaf8729.

19. Zheng, K., Wang, Y., Li, N., Jiang, F.F., Wu, C.X., Liu, F., Chen, H.C., and Liu, Z.F. (2018). Highly efficient base editing in bacteria using a Cas9-cytidine deaminase fusion. Commun. Biol. *1*, 32. https://doi.org/10.1038/s42003-018-0035-5.

20. Li, G., Liu, Y., Zeng, Y., Li, J., Wang, L., Yang, G., Chen, D., Shang, X., Chen, J., Huang, X., and Liu, J. (2017). Highly efficient and precise base editing in discarded human tripronuclear embryos. Protein Cell *8*, 776–779. https://doi.org/10.1007/s13238-017-0458-7.

21. Kang, B.C., Yun, J.Y., Kim, S.T., Shin, Y., Ryu, J., Choi, M., Woo, J.W., and Kim, J.S. (2018). Precision genome engineering through adenine base editing in plants. Nat. Plants *4*, 427–431. https://doi.org/10.1038/s41477-018-0178-x.

22. Tondeur, M., Libert, J., Vamos, E., Van Hoof, F., Thomas, G.H., and Strecker, G. (1982). Infantile form of sialic acid storage disorder: clinical, ultrastructural, and biochemical studies in two siblings. Eur. J. Pediatr. *139*, 142–147. https://doi.org/10.1007/BF00441499.

23. Doench, J.G., Fusi, N., Sullender, M., Hegde, M., Vaimberg, E.W., Donovan, K.F., Smith, I., Tothova, Z., Wilen, C., Orchard, R., et al. (2016). Optimized sgRNA design to maximize activity and minimize off-target effects of CRISPR-Cas9. Nat. Biotechnol. *34*, 184–191. https://doi.org/10.1038/nbt.3437.

24. Bae, S., Park, J., and Kim, J.S. (2014). Cas-OFFinder: a fast and versatile algorithm that searches for potential off-target sites of Cas9 RNA-guided endonucleases. Bioinformatics *30*, 1473–1475. https://doi.org/10.1093/bioinformatics/btu048.

25. Clement, K., Rees, H., Canver, M.C., Gehrke, J.M., Farouni, R., Hsu, J.Y., Cole, M.A., Liu, D.R., Joung, J.K., Bauer, D.E., and Pinello, L. (2019). CRISPResso2 provides accurate and rapid genome editing sequence analysis. Nat. Biotechnol. *37*, 224–226. https://doi.org/10.1038/s41587-019-0032-3.

26. Paavola, L.E., Remes, A.M., Harila, M.J., Varho, T.T., Korhonen, T.T., and Majamaa, K. (2015). A 13-year follow-up of Finnish patients with Salla disease. J. Neurodev. Disord. *7*, 20. https://doi.org/10.1186/s11689-015-9116-7.

27. Hu, W., Chi, C., Song, K., and Zheng, H. (2023). The molecular mechanism of sialic acid transport mediated by Sialin. Sci. Adv. *9*, eade8346. https://doi.org/10.1126/sciadv.ade8346.

28. Tsai, S.Q., Nguyen, N.T., Malagon-Lopez, J., Topkar, V.V., Aryee, M.J., and Joung, J.K. (2017). CIRCLE-seq: a highly sensitive *in vitro* screen for genome-wide CRISPR-Cas9 nuclease off-targets. Nat. Methods *14*, 607–614. https://doi.org/10.1038/nmeth.4278.

29. Sabir, M.S., Hackbarth, M.E., Burke, J.D., Garrett, L.J., Elliott, G., Rivas, C., Springer, D.A., Leoyklang, P., Clark, T.S., Huizing, M., et al. (2022). A novel experimental mouse model to investigate a free sialic acid storage disorder (Salla disease). Mol. Genet. Metabol. *135*, S107. https://doi.org/10.1016/j.ymgme.2021.11.283.

30. Hwang, G.H., and Bae, S. (2021). Web-Based Base Editing Toolkits: BE-Designer and BE-Analyzer. Methods Mol. Biol. *2189*, 81–88. https://doi.org/10.1007/978-1-0716-0822-7_7.

31. Kleinstiver, B.P., Prew, M.S., Tsai, S.Q., Topkar, V.V., Nguyen, N.T., Zheng, Z., Gonzales, A.P.W., Li, Z., Peterson, R.T., Yeh, J.R.J., et al. (2015). Engineered CRISPR-Cas9 nucleases with altered PAM specificities. Nature *523*, 481–485. https://doi.org/10.1038/nature14592.

32. Koblan, L.W., Doman, J.L., Wilson, C., Levy, J.M., Tay, T., Newby, G.A., Maianti, J.P., Raguram, A., and Liu, D.R. (2018). Improving cytidine and adenine base editors by expression optimization and ancestral reconstruction. Nat. Biotechnol. *36*, 843–846. https://doi.org/10.1038/nbt.4172.

33. Stirling, D.R., Swain-Bowden, M.J., Lucas, A.M., Carpenter, A.E., Cimini, B.A., and Goodman, A. (2021). CellProfiler 4: improvements in speed, utility and usability. BMC Bioinf. *22*, 433. https://doi.org/10.1186/s12859-021-04344-9.

34. Schindelin, J., Arganda-Carreras, I., Frise, E., Kaynig, V., Longair, M., Pietzsch, T., Preibisch, S., Rueden, C., Saalfeld, S., Schmid, B., et al. (2012). Fiji: an open-source platform for biological-image analysis. Nat. Methods *9*, 676–682. https://doi.org/10.1038/nmeth.2019.

35. Lemyre, E., Russo, P., Melançon, S.B., Gagné, R., Potier, M., and Lambert, M. (1999). Clinical spectrum of infantile free sialic acid storage disease. Am. J. Med. Genet. *82*, 385–391.